

## Article

# An Impact Assessment of a Transportable BESS on the Protection of Conventional Distribution Systems

Antonio E. C. Momesso <sup>1,\*</sup>, Pedro H. A. Barra <sup>2</sup>, Pedro I. N. Barbalho <sup>3</sup>, Eduardo N. Asada <sup>3</sup>,  
José C. M. Vieira <sup>3</sup> and Denis V. Coury <sup>3</sup>

<sup>1</sup> Electrical Engineering Department, Faculty of Architecture, Engineering and Technology, Federal University of Mato Grosso, Cuiabá 78060-900, Brazil

<sup>2</sup> Faculty of Electrical Engineering, Federal University of Uberlândia, Uberlândia 38400-902, Brazil; pedrobarra@ufu.br

<sup>3</sup> Department of Electrical and Computer Engineering, São Carlos School of Engineering, University of São Paulo, São Carlos 13566-590, Brazil; pedro.inacio.barbalho@usp.br (P.I.N.B.); easada@usp.br (E.N.A.); jcarlos@sc.usp.br (J.C.M.V.); coury@sc.usp.br (D.V.C.)

\* Correspondence: antonio.momesso@ufmt.br

**Abstract:** The integration of new battery technologies has become a focal point for distribution utilities, driven by decreasing costs and the need for fast responsiveness. Transportable battery energy storage systems (TBESSs) offer additional flexibility, allowing connection at multiple substations or grid feed points. However, concerns remain regarding their impact on distribution systems (DSs), particularly on protection devices (PDs). This study addresses these concerns by investigating the influence of TBESSs on the protection systems of a real-world distribution network. Given the lack of studies in the current literature on this topic, this research aims to fill this gap by examining the potential effects of TBESS integration on PDs, such as reclosers and fuses, within a DS. Utilizing a model based on real data from a Brazilian utility, we conducted simulations to analyze the effects of TBESSs in both charging and discharging modes on the protection systems of three feeders. The methodology involved assessing variations in the operation times and coordination of PDs to determine if TBESS integration would necessitate adjustments to existing protection configurations. The results demonstrated that TBESS integration resulted in only minor variations in PD operating times, typically within hundredths of a second, indicating a negligible impact on protection performance. Consequently, no significant modifications to the protection system are required to accommodate TBESSs. These findings suggest that TBESSs can be seamlessly integrated into existing distribution networks, maintaining system reliability and operational integrity. This study provides valuable insights and a robust procedure for utilities to analyze the integration of TBESSs, supporting the effective deployment of modern energy storage solutions in DSs.

**Keywords:** distribution system; power system simulation; protection; short-circuit; transportable energy storage system



**Citation:** Momesso, A.E.C.; Barra, P.H.A.; Barbalho, P.I.N.; Asada, E.N.; Vieira, J.C.M.; Coury, D.V. An Impact Assessment of a Transportable BESS on the Protection of Conventional Distribution Systems. *Energies* **2024**, *17*, 4196. <https://doi.org/10.3390/en17164196>

Academic Editor: Santi A. Rizzo

Received: 26 June 2024

Revised: 22 July 2024

Accepted: 26 July 2024

Published: 22 August 2024



**Copyright:** © 2024 by the authors. Licensee MDPI, Basel, Switzerland. This article is an open access article distributed under the terms and conditions of the Creative Commons Attribution (CC BY) license (<https://creativecommons.org/licenses/by/4.0/>).

## 1. Introduction

Energy storage systems (ESSs) have increasingly attracted utilities due to their relevant characteristics, such as declining costs and fast response [1]. Moreover, concerns about decarbonization have also driven the utilization of ESSs [2]. Among the various energy storage technologies, battery energy storage systems (BESSs) stand out as an attractive solution, providing adaptability, fast response, controllability, geographical independence, and environmental friendliness [3,4].

In distribution systems (DSs), the BESS is suitable for various applications, ranging from short-term to long-term ones, such as peak shaving, frequency and voltage control, power loss reduction, and energy management [5]. The success of BESSs in these applications is due to recent research, which enriches the understanding of battery behavior

throughout its life cycle and presents new solutions to improve its performance [6]. In recent years, these applications have become more flexible through transportable battery energy storage systems (TBESSs). In this alternative solution, all components are packed in a container and mobilized by a truck. Thus, the distribution utility can plan the solution's connection at different power substations or points on the feeder for various purposes [7].

Globally, practical applications of TBESSs have demonstrated their versatility. In Brazil, for example, there was a call for strategic R&D projects to promote power storage projects nationally—call no. 21/2016 by the Brazilian Electricity Regulatory Agency (ANEEL). One approved project includes a 1 MW/1 MWh TBESS to assist with scheduled contingencies at substations. Another example is the application of a 500 kW/1 MWh TBESS connected to a tea factory in China, used for peak shaving [7].

Some studies in the literature aim to support the effective implementation of TBESSs. For instance, reference [8] presented a TBESS routing and scheduling strategy for DSs considering survivability and recovery. Reference [9] developed a routing approach to avoid possible load shedding caused by disasters, while reference [10] used a multi-objective mixed-integer linear programming framework to schedule TBESSs in power systems. Conversely, the techno-economic impacts of TBESSs on the scheduling of power systems were investigated by [11,12]. Other studies, such as reference [13,14], explored the planning, operation, and management of TBESSs in the context of electric vehicle charging stations, and reference [15] proposed a new scheduling model to minimize curtailed renewable energy by absorbing and releasing excess energy where and when required, considering the distribution context. Reference [16] developed a resilience-driven planning model for the optimal sizing and location of TBESSs considering networked microgrids. Similarly, reference [17] proposed a multi-agent-based strategy for routing and scheduling TBESSs. Finally, considering the microgrids' context integrating TBESSs, the authors of [18] proposed a quantification framework to evaluate the resilience of distribution networks.

In the literature, there are also works assessing the impact of BESSs in power systems. For instance, Ref. [19] analyzes the operation of a lithium-ion battery technology based on a 1 MW/1.29 MWh BESS connected in parallel with wind generation with a capacity of 50.4 MW, focusing on power smoothing and power factor correction. Article [20] examines the mitigation of harmonic components derived from non-linear loads through BESSs. Finally, article [21] conducts various studies in steady and transient states to observe the impact of BESS connections, mainly on DS voltage. If the search includes inverter-based resources, articles such as [22], which addresses the impact of inverter-based generators on distance protection, can be found. Additionally, the authors in [23] studied the impact of inverter-based features on various protection schemes, from distance protection to line differential protection. However, there is a lack of studies on the influence of BESS connections on protection systems, particularly those already existing on real feeders.

In a previous study [24], the authors investigated the impacts of a TBESS on the short-circuit behavior of a DS. Using a test feeder found in the literature, they concluded that the TBESS connection, whether charging or discharging, slightly modified the short-circuit currents observed by the DS's protection device (PD). However, this study was limited to short-circuit currents and did not explore the protection aspect. Additionally, it considered a simple test feeder and non-practical data. This raises new questions: Would this modification in short-circuit behavior be sufficient to cause problems for the existing protection system settings? Would these impacts affect the coordination between PDs?

In this context, this paper presents an analysis of the influence of TBESS connections on the existing power system protection of a DS, considering real-world elements such as substations, feeders, PDs and their adjustments, and TBESS data. All elements were modeled in PSCAD™/EMTDC™ to generate the simulations analyzed in this paper. It is worth mentioning that, as part of an R&D project, all models were validated and built based on data from manufacturers and the utility company. This meticulous approach ensured that the simulation faithfully mirrored the actual system operation, encompass-

ing everything from load behavior to battery performance, thus replicating real-world measurements accurately.

The main objective is to determine whether the TBESS connection (charging or discharging) can cause concerns regarding the existing protection system settings. Additionally, the analysis considers the impacts on the coordination between PDs (e.g., recloser–recloser and recloser–fuse coordination). Thus, the novelty and main contributions of this paper include the following:

- An investigation into the impacts of TBESSs on existing protection systems in distribution utilities, a topic not previously studied.
- Analyses based on practical and real-world elements, including three large feeders with 582 nodes, 11 reclosers, and 120 fuses, using real-world feeder protection settings.
- Insights for further investigations by other distribution utilities and potential applications of the proposed methodology to analyze different systems or connection points.

It should also be noted that some standards, such as IEEE 1547-2018 [25], require that distributed resources remain connected to the system even during transient conditions to support the network. Thus, this study aligns with these standards and is important because the permanence of distributed resources, such as TBESSs, can influence short-circuit currents and, consequently, lead to the improper performance of PDs, potentially isolating a larger part of the system than necessary.

The remainder of this paper is arranged as follows. Section 2 details the methodology used for the analysis, emphasizing the modeled distribution feeders and the TBESS. Section 3 presents the results and analyses. Finally, Section 4 concludes the paper.

## 2. Methodology

This section describes the analyzed feeders, providing relevant information concerning their protection. After that, the TBESS model and the characterization of the simulated faults are presented.

### 2.1. Analyzed Feeders

During the studies, a real DS from a Brazilian utility was used. The DS was modeled and validated using data (for lines, transformers, loads, PDs, and short-circuit levels) provided by the utility. This system comprised three feeders, designated as feeders #1, #2, and #3. Feeder #1 (Figure 1) had a total length of 117.95 km and a load of 447 kVA, with 3 reclosers and 23 fuses used for protection purposes. Feeder #2 (Figure 2) had a length of 75.07 km, a load of 236 kVA, and was protected by 3 reclosers and 18 fuses. Finally, feeder #3 (Figure 3), with a length of 136.81 km and a load of 1603 kVA, was protected by 5 reclosers and 80 fuses.

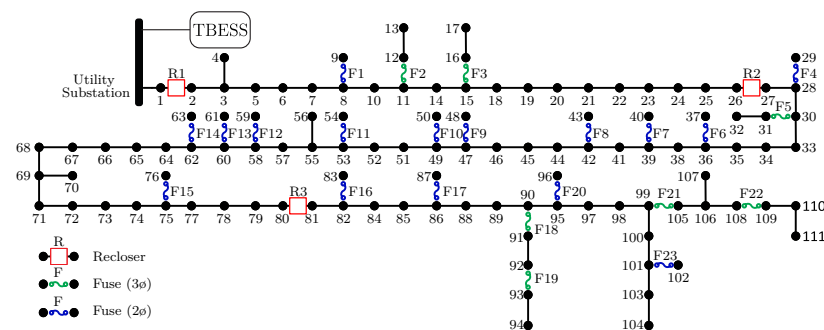


Figure 1. Analyzed real feeder—feeder #1.

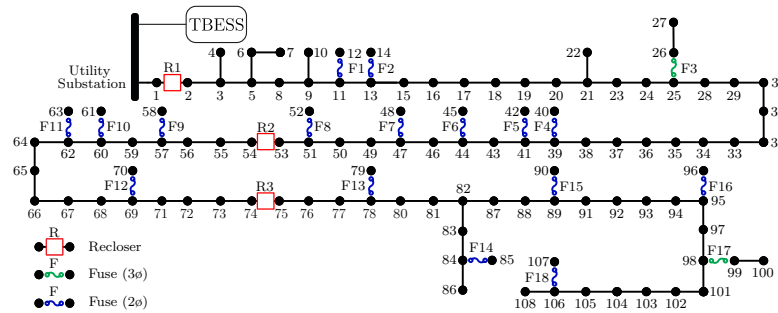


Figure 2. Analyzed real feeder—feeder #2.

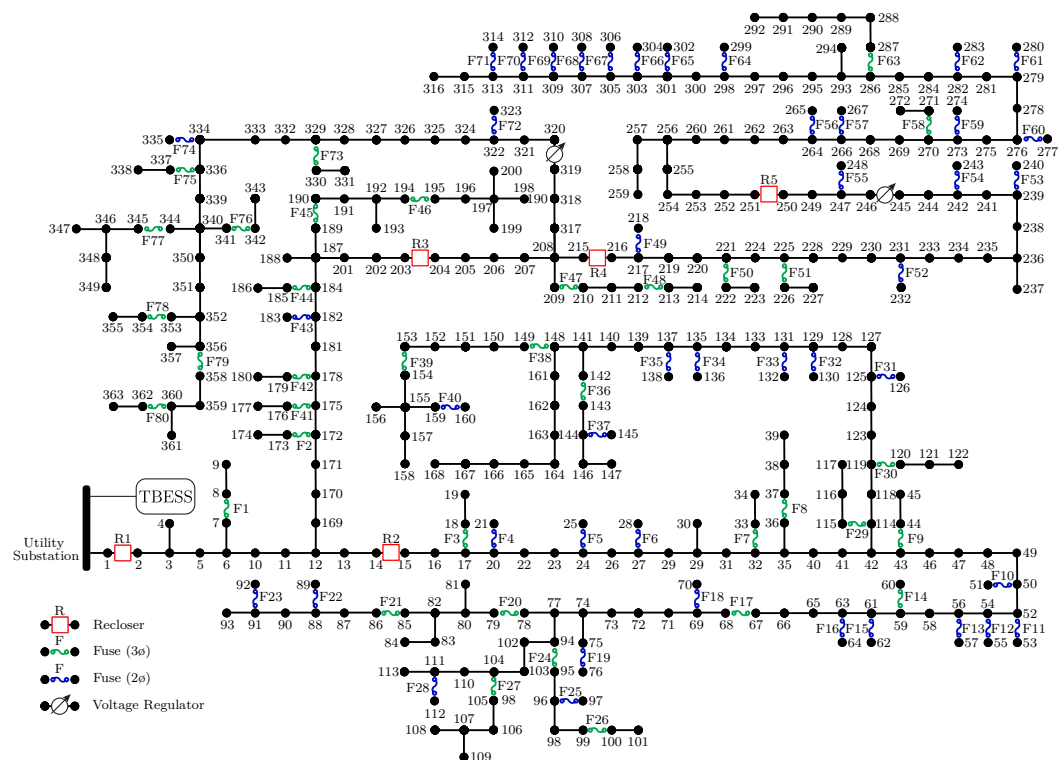


Figure 3. Analyzed real feeder—feeder #3.

It is important to highlight that the three feeders were fed through a 34.5 kV/13.8 kV, 2.5 MVA transformer (YNd1) with a short-circuit level of 37 MVA. Moreover, the 13.8 kV substation side was grounded by a grounding transformer with a zigzag connection and an impedance of  $7.97 \Omega$ . The voltage regulators of feeder #3 had an open delta connection, and their taps were fixed during all short-circuit simulations. The constant power model was considered for loads. Additionally, it is important to mention that loads with a voltage below 0.8 pu were converted to constant impedance load models during the faults.

Concerning the protection information, Tables 1 and 2 present the data of the PDs in the feeders (Figures 1–3). It should be noted that Table 1 shows information about the fuses, including their current and type. Table 2 presents data about the reclosers, including the current transformer ratio, the pickup values, and details about the Cooper curve [26]. These data comprise the actual settings of the protection system informed by the utility.

**Table 1.** Nominal current and type of allocated fuses.

Current and Type	Fuse	Current and Type	Fuse
Feeder #1			
6 K	F5, F7, F20, F23	10 K	F6, F9, F10, F12, F13, F14, F16, F18, F19
15 K	F4, F8, F17, F22	25 K	F1, F2, F3, F21
200 K	F11, F15		
Feeder #2			
6 K	F1, F6, F14, F16, F18	10 K	F2, F4, F5, F12, F13, F15, F17
15 K	F3, F7, F8, F9, F10, F11		
Feeder #3			
10 K	F1, F2, F3, F4, F5, F6, F9, F10, F11, F14, F15, F16, F19, F20, F21, F22, F25, F26, F27, F29, F30, F32, F33, F34, F35, F36, F38, F40, F41, F46, F51, F52, F53, F54, F57, F58, F59, F60, F62, F63, F64, F65, F66, F67, F73, F77, F78, F80	1 H	F61
		2 H	F7
		3 H	F48
		6 K	F12, F13, F23, F24, F31, F37, F39, F50, F55, F56, F68, F69, F70, F71, F75
		15 K	F17, F42, F79
		25 K	F8, F43, F44, F45, F47, F49, F72, F74, F76
		200 K	F18, F28

**Table 2.** Data of the reclosers allocated.

Recloser	Current Transformer	Pickup Current	Curve	Time Dial	Time Adder
Feeder #1—phase					
R1	400:1	150 A	133	2	0.05
R2	1000:1	80 A	133	1.9	0
R3	1000:1	80 A	133	1.4	0
Feeder #1—neutral					
R1	400:1	20 A	131	1	0
R2	1000:1	20 A	131	0.8	0
R3	1000:1	20 A	131	0.6	0
Feeder #2—phase					
R1	400:1	160 A	120	1.9	0
R2	1000:1	100 A	136	0.8	0.1
R3	1000:1	100 A	136	0.6	0
Feeder #2—neutral					
R1	400:1	25 A	140	1	0.1
R2	1000:1	25 A	140	0.8	0
R3	1000:1	25 A	140	0.6	0
Feeder #3—phase					
R1	400:1	160 A	120	1.9	0
R2	1000:1	130 A	136	1.2	0.1
R3	1000:1	160 A	120	1.2	0
R4	1000:1	100 A	136	1.4	0
R5	1000:1	100 A	136	0.4	0
Feeder #3—neutral					
R1	400:1	25 A	140	1	0.1
R2	1000:1	25 A	140	0.83	0
R3	1000:1	25 A	140	0.85	0
R4	1000:1	25 A	140	0.6	0
R5	1000:1	25 A	140	0.4	0

Equation (1) [26] presents the calculation of the recloser tripping time, where the coefficients  $A$ ,  $B$ ,  $C$ , and  $p$  are given by the curve used (shown in Table 3),  $I_{rms}$  is the current measured by the recloser,  $I_{pickup}$  is the pickup current,  $TD$  is the time dial, and  $TS$  is the time adder:

$$t_{trip} = \left[ \frac{A}{\left( \frac{I_{rms}}{I_{pickup}} \right)^p - C} + B \right] \times TD + TS \quad (1)$$

**Table 3.** Data of the curves adopted [26].

Curve	A	B	C	p
120	6.04	0.086	0.362	1.867
131	7.767	5.299	−0.26	2.002
133	10.251	0.032	0.282	1.915
136	Interpolated curve			
140	15.341	0.853	0.432	1.74

As for the operating times of the fuses, these were obtained from the points on the curve provided by the manufacturer [27]. Based on the fault current value measured by the fuse, the respective maximum and minimum operation times were found through interpolation of the adjacent points.

## 2.2. TBESS Model

Figure 4 depicts the TBESS modeled in this work. This model comprised a battery bank with a 1 MWh capacity and 1 MW rated power, a DC–DC converter, a voltage-sourced converter (VSC), an LCL filter, and a transformer rated at 2 MVA, 1 kV/13.8 kV, with an 8% reactance. The DC–DC buck–boost converter controlled the battery bank output power, regulating whether it injects or stores energy. In this context, the VSC, operating at a switching frequency of 10 kHz, maintained a constant 4 kV DC link voltage by managing the active power exchanged with the AC grid. Additionally, the VSC controlled the output reactive power of the TBESS. The LCL filter is designed to dampen the harmonics of the VSC output current and consists of a converter-side inductor ( $L_1 = 1.4$  mH), a grid-side inductor ( $L_2 = 667.84$   $\mu$ H), and a capacitor between both inductors ( $C_f = 33.16$   $\mu$ F).

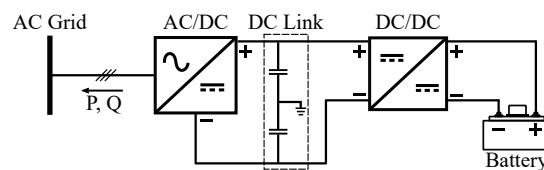


**Figure 4.** TBESS model.

It is worth mentioning that, during the applied faults, the TBESS was controlled to maintain a constant power injection or absorption with a unity power factor. The discharge power of the TBESS was set at 1 MW, and the recharge power was set at 0.5 MW. Additionally, although the TBESS is set to keep constant active and reactive power injection/absorption, the controller tries to limit the output current to 2 pu. This feature is crucial when the TBESS is connected to a grid and the terminal AC voltage drops significantly, as in fault situations. The controller acts to maintain constant power, but when the grid voltage drops, the TBESS current tends to increase, potentially damaging the converter components.

### 2.3. Performed Analyses

An interface between PSCAD™/EMTDC™ and the *Python* programming language was used to automate the simulations. This setup allowed for the modification of simulation parameters, such as fault location and the operation mode of the TBESS, thereby generating a comprehensive set of simulations.

The eleven fault types (single-phase to ground, two-phase, two-phase to ground, three-phase, and three-phase to ground) were applied on the downstream bus closest to the PD. The fault resistance was adjusted to  $0.01 \Omega$ . Therefore, 2760 fault simulations were analyzed: 920 (174, 119, and 627 faults on feeders #1, #2, and #3, respectively) considering the TBESS discharging, 920 for charging, and another 920 without the TBESS (reference situation).

For each fault applied, the operating time of each PD involved was recorded. These times were analyzed to determine whether the TBESS, during its charging or discharging, impacted the protection system. Specifically, we checked whether a device that previously had a given operating time experienced an increase or reduction with TBESS allocation, which could cause a loss of selectivity. Additionally, we intended to analyze whether the PDs remained coordinated according to the condition specified in Equation (2) [28].

$$t_{backup} - t_{primary} \geq CTI \quad (2)$$

where  $t_{backup}$  is the operating time of the backup device,  $t_{primary}$  is the operating time of the device closest to the fault, and  $CTI$  is the coordination time interval, adopted as 200 ms.

It is worth mentioning that, in this study, the fuse was the primary actuation element, with the recloser serving as a backup device. Therefore, the fuse-blowing philosophy was adopted. The CTI can be obtained between the maximum operating time of the fuse (found through interpolation) and the operating time of the recloser (calculated using Equation (1)), or between the maximum operating time of the downstream fuse and the minimum operating time of the upstream fuse (both obtained through interpolation), or between the operating time of the upstream recloser and the downstream recloser (both calculated using Equation (1)).

## 3. Results

The following subsections present the analyses for each investigated feeder. The results are shown both graphically and statistically by comparing the reference behavior of the protection system with the new behavior when the TBESS is operating (charging or discharging). The investigations focused on the operating times of the existing reclosers and fuses, as well as the CTI between these PDs (recloser–recloser, recloser–fuse, and fuse–fuse).

### 3.1. Analysis of Feeder #1

Table 4 presents a statistical analysis of the operating times of the PDs, with and without the TBESS in charging mode. When comparing the times shown in this table, there is no noticeable significant impact when placing the TBESS in charging mode (cases with pronounced changes are highlighted in bold). This suggests that the integration of the TBESS in charging mode does not significantly affect the performance of most PDs. Generally, variations of only a few hundredths of a second are observed in reclosers and fuses F2, F14, F17, and F21. The most significant difference found is 0.16 s in the operating time of recloser R1 when a BC fault is applied at bus 109.

Notably, fuses F11 and F15 do not operate in either case because both are 200 K fuses, which start to act at 480 A, while the fault current reaches a maximum value of only 377 A. In this situation, it would be necessary to replace them with 25K fuses, which start operating at 40 A, to ensure that protection is not carried out exclusively by the recloser. Furthermore, times greater than 10 s were obtained by recloser R1 for faults at the end of the feeder. These times are satisfactory, since it is the third backup device.

**Table 4.** Statistical evaluation of the operating times of PDs with and without the TBESS in charging mode (feeder #1).

PD	Operating Time (s)									
	With TBESS					Without TBESS				
	Min.	25th Perc.	50th Perc.	75th Perc.	Max.	Min.	25th Perc.	50th Perc.	75th Perc.	Max.
<b>R1</b>	<b>0.35</b>	<b>1.93</b>	5.34	5.49	<b>18.78</b>	<b>0.34</b>	<b>1.91</b>	5.34	5.49	<b>18.62</b>
<b>R2</b>	0.43	<b>1.24</b>	<b>2.44</b>	<b>3.76</b>	<b>5.03</b>	0.43	<b>1.22</b>	<b>2.42</b>	<b>3.73</b>	<b>4.99</b>
<b>R3</b>	<b>1.50</b>	<b>2.32</b>	<b>2.98</b>	3.26	<b>4.10</b>	<b>1.48</b>	<b>2.30</b>	<b>2.95</b>	3.26	<b>4.07</b>
F1	0.06	0.07	0.09	0.13	0.16	0.06	0.07	0.09	0.13	0.16
<b>F2</b>	0.06	0.07	0.08	0.09	<b>0.17</b>	0.06	0.07	0.08	0.09	<b>0.16</b>
F3	0.06	0.07	0.08	0.09	0.18	0.06	0.07	0.08	0.09	0.18
F4	0.06	0.06	0.08	0.09	0.12	0.06	0.06	0.08	0.09	0.12
F5	0.05	0.05	0.06	0.06	0.07	0.05	0.05	0.06	0.06	0.07
F6	0.05	0.05	0.07	0.07	0.09	0.05	0.05	0.07	0.07	0.09
F7	0.05	0.05	0.06	0.06	0.07	0.05	0.05	0.06	0.06	0.07
F8	0.07	0.07	0.09	0.11	0.14	0.07	0.07	0.09	0.11	0.14
F9	0.06	0.06	0.08	0.08	0.10	0.06	0.06	0.08	0.08	0.10
F10	0.06	0.06	0.08	0.08	0.10	0.06	0.06	0.08	0.08	0.10
F12	0.06	0.06	0.08	0.08	0.11	0.06	0.06	0.08	0.08	0.11
F13	0.06	0.07	0.08	0.09	0.11	0.06	0.07	0.08	0.09	0.11
<b>F14</b>	0.06	0.07	<b>0.09</b>	0.09	0.11	0.06	0.07	<b>0.08</b>	0.09	0.11
F16	0.08	0.09	0.11	0.12	0.15	0.08	0.09	0.11	0.12	0.15
<b>F17</b>	0.16	0.17	<b>0.21</b>	0.23	0.29	0.16	0.17	<b>0.20</b>	0.23	0.29
F18	0.08	0.09	0.11	0.12	0.16	0.08	0.09	0.11	0.12	0.16
F19	0.08	0.09	0.11	0.12	0.16	0.08	0.09	0.11	0.12	0.16
F20	0.07	0.07	0.08	0.09	0.11	0.07	0.07	0.08	0.09	0.11
<b>F21</b>	<b>0.39</b>	0.50	<b>0.58</b>	<b>0.68</b>	<b>1.05</b>	<b>0.38</b>	0.50	<b>0.57</b>	<b>0.67</b>	<b>1.04</b>
F22	0.19	0.23	0.25	0.30	0.42	0.19	0.23	0.25	0.30	0.42
F23	0.07	0.07	0.09	0.10	0.12	0.07	0.07	0.09	0.10	0.12

As expected, when the TBESS changes its operating mode to discharge (Table 5), the operating time of the PDs slightly decreases. Again, when observing the values in the table, changes are observed only in the times of reclosers and fuses F1, F3, F9, F17, and F21. Moreover, the BC fault on bus 109 presents the most notable difference (0.28 s) in the recloser R1 time. Finally, it is verified that, even with the TBESS contributing to the fault, fuses F11 and F15 do not operate, since, even though the current reaches 382 A in this case, it is still not enough to activate the fuses.

**Table 5.** Statistical evaluation of the operating times of PDs with and without the TBESS in discharge mode (feeder #1).

PD	Operating Time (s)									
	With TBESS					Without TBESS				
	Min.	25th Perc.	50th Perc.	75th Perc.	Max.	Min.	25th Perc.	50th Perc.	75th Perc.	Max.
<b>R1</b>	<b>0.32</b>	<b>1.88</b>	5.34	<b>5.48</b>	<b>18.34</b>	<b>0.34</b>	<b>1.91</b>	5.34	<b>5.49</b>	<b>18.62</b>
<b>R2</b>	<b>0.42</b>	<b>1.21</b>	<b>2.39</b>	<b>3.68</b>	<b>4.92</b>	<b>0.43</b>	<b>1.22</b>	<b>2.42</b>	<b>3.73</b>	<b>4.99</b>
<b>R3</b>	<b>1.46</b>	<b>2.27</b>	<b>2.91</b>	<b>3.25</b>	<b>4.01</b>	<b>1.48</b>	<b>2.30</b>	<b>2.95</b>	<b>3.26</b>	<b>4.07</b>
F1	0.06	0.07	<b>0.08</b>	0.13	0.16	0.06	0.07	<b>0.09</b>	0.13	0.16
F2	0.06	0.07	0.08	0.09	0.16	0.06	0.07	0.08	0.09	0.16
<b>F3</b>	0.06	0.07	0.08	0.09	<b>0.17</b>	0.06	0.07	0.08	0.09	<b>0.18</b>
F4	0.06	0.06	0.08	0.09	0.12	0.06	0.06	0.08	0.09	0.12

Table 5. Cont.

PD	Operating Time (s)									
	With TBESS					Without TBESS				
	Min.	25th Perc.	50th Perc.	75th Perc.	Max.	Min.	25th Perc.	50th Perc.	75th Perc.	Max.
F5	0.05	0.05	0.06	0.06	0.07	0.05	0.05	0.06	0.06	0.07
F6	0.05	0.05	0.07	0.07	0.09	0.05	0.05	0.07	0.07	0.09
F7	0.05	0.05	0.06	0.06	0.07	0.05	0.05	0.06	0.06	0.07
F8	0.07	0.07	0.09	0.11	0.14	0.07	0.07	0.09	0.11	0.14
<b>F9</b>	0.06	0.06	<b>0.07</b>	0.08	0.10	0.06	0.06	<b>0.08</b>	0.08	0.10
F10	0.06	0.06	0.08	0.08	0.10	0.06	0.06	0.08	0.08	0.10
F12	0.06	0.06	0.08	0.08	0.11	0.06	0.06	0.08	0.08	0.11
F13	0.06	0.07	0.08	0.09	0.11	0.06	0.07	0.08	0.09	0.11
F14	0.06	0.07	0.08	0.09	0.11	0.06	0.07	0.08	0.09	0.11
F16	0.08	0.09	0.11	0.12	0.15	0.08	0.09	0.11	0.12	0.15
<b>F17</b>	<b>0.15</b>	0.17	0.20	0.23	0.29	<b>0.16</b>	0.17	0.20	0.23	0.29
F18	0.08	0.09	0.11	0.12	0.16	0.08	0.09	0.11	0.12	0.16
F19	0.08	0.09	0.11	0.12	0.16	0.08	0.09	0.11	0.12	0.16
F20	0.07	0.07	0.08	0.09	0.11	0.07	0.07	0.08	0.09	0.11
<b>F21</b>	0.38	<b>0.49</b>	<b>0.56</b>	<b>0.66</b>	<b>1.03</b>	0.38	<b>0.50</b>	<b>0.57</b>	<b>0.67</b>	<b>1.04</b>
F22	0.19	0.23	0.25	0.30	0.42	0.19	0.23	0.25	0.30	0.42
F23	0.07	0.07	0.09	0.10	0.12	0.07	0.07	0.09	0.10	0.12

Figure 5 shows the boxplots of the CTIs between the PDs with and without the TBESS. It is observed that the CTIs are much larger between reclosers R2 and R1 than between R3 and R2. Since the CTIs between fuses F1, F2, F3, and recloser R1 are also high, this indicates that the operating time of recloser R1 could be reduced through its reparameterization. In general, the intervals are primarily below 3 s when considering coordination between reclosers and fuses, and a reduction in the operating time of recloser R3 is also possible. Regarding the coordination between fuses, the selectivity is non-existent between fuses F19 and F18 in the system without the TBESS, which requires the replacement of fuse F18 with a larger capacity one. This pattern is sustained in the cases with the TBESS. Additionally, in some cases, there is a loss of coordination between F22 and F21 when considering a CTI reference of 200 ms. Finally, the behavior of the CTI does not change with the TBESS allocation. There is a slight increase in CTIs with the TBESS in charge mode. In discharge mode, there is a minimal reduction in the interval.

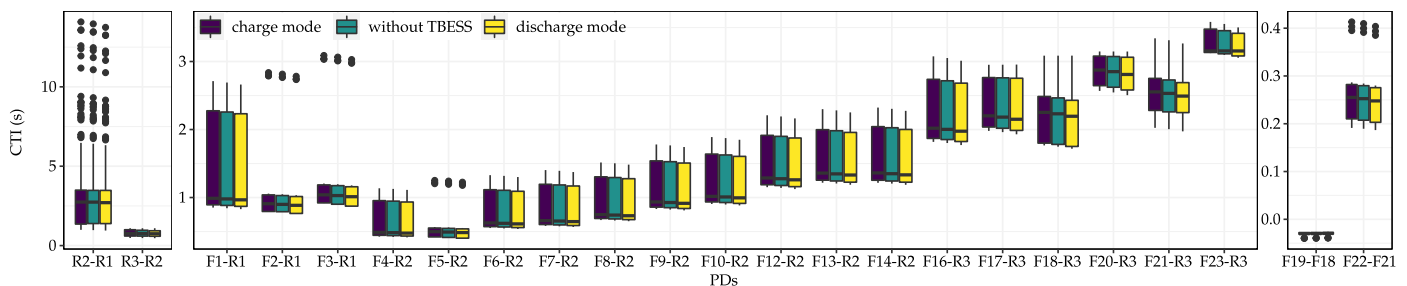


Figure 5. Boxplot of the CTIs obtained between the PDs with and without the TBESS (feeder #1).

The minor impact of the TBESS can be explained by the ratio between its maximum power and the short-circuit ratio of the substation. While the TBESS provided 1 MW during discharge and 0.5 MW for recharge, the substation short-circuit level is 37 MVA. Moreover, the TBESS was controlled by a power converter, which limited its current to 2 pu. Thus, it was expected to have a small contribution to the short-circuit current and, consequently, to the PDs' operating times. It is worth mentioning that feeder #1 comprised

an intermediate level of load and length. The following analysis elucidates the difference in the PDs' operating times for feeders with different lengths and load levels.

### 3.2. Analysis of Feeder #2

Table 6 presents the statistical analysis of the operating times of PDs with and without the TBESS in charging mode, considering feeder #2. As can be seen, there is a slight variation only in reclosers and in the times of fuses F5, F14, and F17. For this feeder, the most significant time difference obtained for the TBESS in charging mode is 0.14 s in recloser R1 when an AC fault on bus 107 is applied.

**Table 6.** Statistical evaluation of the operating times of PDs with and without the TBESS in charging mode (feeder #2).

PD	Operating Time (s)									
	With TBESS					Without TBESS				
	Min.	25th Perc.	50th Perc.	75th Perc.	Max.	Min.	25th Perc.	50th Perc.	75th Perc.	Max.
<b>R1</b>	<b>0.33</b>	1.19	1.42	<b>2.03</b>	<b>15.08</b>	<b>0.32</b>	1.19	1.42	<b>2.02</b>	<b>14.94</b>
<b>R2</b>	<b>0.69</b>	0.91	<b>1.23</b>	<b>1.54</b>	<b>3.39</b>	<b>0.68</b>	0.91	<b>1.22</b>	<b>1.53</b>	<b>3.37</b>
<b>R3</b>	0.79	<b>0.94</b>	1.03	<b>1.27</b>	<b>2.53</b>	0.79	<b>0.93</b>	1.03	<b>1.26</b>	<b>2.51</b>
F1	0.05	0.05	0.05	0.05	0.06	0.05	0.05	0.05	0.05	0.06
F2	0.05	0.05	0.05	0.05	0.07	0.05	0.05	0.05	0.05	0.07
F3	0.05	0.06	0.07	0.08	0.12	0.05	0.06	0.07	0.08	0.12
F4	0.05	0.05	0.07	0.07	0.09	0.05	0.05	0.07	0.07	0.09
<b>F5</b>	0.05	<b>0.07</b>	0.07	<b>0.08</b>	0.09	0.05	<b>0.05</b>	0.07	<b>0.07</b>	0.09
F6	0.05	0.05	0.06	0.06	0.07	0.05	0.05	0.06	0.06	0.07
F7	0.08	0.08	0.10	0.12	0.15	0.08	0.08	0.10	0.12	0.15
F8	0.08	0.08	0.11	0.12	0.16	0.08	0.08	0.11	0.12	0.15
F9	0.08	0.09	0.11	0.13	0.16	0.08	0.09	0.11	0.13	0.16
F10	0.09	0.09	0.11	0.13	0.17	0.09	0.09	0.11	0.13	0.17
F11	0.09	0.10	0.12	0.14	0.18	0.09	0.10	0.12	0.14	0.18
F12	0.07	0.08	0.10	0.10	0.13	0.07	0.08	0.10	0.10	0.13
F13	0.09	0.10	0.12	0.13	0.16	0.09	0.10	0.12	0.13	0.16
<b>F14</b>	0.07	0.08	<b>0.10</b>	<b>0.11</b>	0.13	0.07	0.08	<b>0.09</b>	<b>0.10</b>	0.13
F15	0.10	0.11	0.13	0.14	0.17	0.10	0.11	0.13	0.14	0.17
F16	0.07	0.07	0.09	0.10	0.11	0.07	0.07	0.09	0.10	0.11
<b>F17</b>	0.10	0.11	0.13	<b>0.15</b>	0.19	0.10	0.11	0.13	<b>0.14</b>	0.19
F18	0.07	0.08	0.09	0.11	0.12	0.07	0.08	0.09	0.11	0.12

In discharge mode (Table 7), a reduction in the operating times of reclosers and fuses F9, F10, and F14 is observed. The most significant difference is noted in recloser R1 due to an AC fault on bus 107 (0.25 s). As in feeder #1, this small difference in times indicates that it is not necessary to adjust the existing protection system to accommodate the TBESS. However, unlike feeder #1, these simulations do not show any cases of non-sensitization of protection. In addition, it is noted that the operating times of recloser R1 are greater than 10 s for faults at the end of the feeder.

Figure 6 presents the CTIs obtained between the PDs for the three simulation sets considered. Again, the most considerable intervals are observed between reclosers R1 and R2. In this case, it is impossible to reduce the actuation time of recloser R1, since the CTI between, for example, fuse F1 and recloser R1 is already low. Regarding feeder #1, there is a slight reduction in the CTIs between reclosers and fuses. There is no loss of selectivity or coordination, assuming a CTI of 200 ms. Finally, there is a small reduction in the CTI when the TBESS is in discharge mode and a small increase when in charge mode.

The TBESS's power was about four times greater than the feeder #2 loads. However, this penetration level was insufficient to jeopardize the PDs' operation. Thus, feeder #3 was

analyzed to understand the TBESS’s impact on a system with a much greater length and load level.

**Table 7.** Statistical evaluation of the operating times of PDs with and without the TBESS in discharge mode (feeder #2).

PD	Operating Time (s)									
	With TBESS					Without TBESS				
	Min.	25th Perc.	50th Perc.	75th Perc.	Max.	Min.	25th Perc.	50th Perc.	75th Perc.	Max.
<b>R1</b>	<b>0.31</b>	1.19	<b>1.41</b>	<b>2.00</b>	<b>14.69</b>	<b>0.32</b>	1.19	<b>1.42</b>	<b>2.02</b>	<b>14.94</b>
<b>R2</b>	<b>0.67</b>	0.91	1.22	<b>1.52</b>	<b>3.33</b>	<b>0.68</b>	0.91	1.22	<b>1.53</b>	<b>3.37</b>
<b>R3</b>	<b>0.78</b>	<b>0.92</b>	<b>1.02</b>	<b>1.25</b>	<b>2.48</b>	<b>0.79</b>	<b>0.93</b>	<b>1.03</b>	<b>1.26</b>	<b>2.51</b>
F1	0.05	0.05	0.05	0.05	0.06	0.05	0.05	0.05	0.05	0.06
F2	0.05	0.05	0.05	0.05	0.07	0.05	0.05	0.05	0.05	0.07
F3	0.05	0.06	0.07	0.08	0.12	0.05	0.06	0.07	0.08	0.12
F4	0.05	0.05	0.07	0.07	0.09	0.05	0.05	0.07	0.07	0.09
F5	0.05	0.05	0.07	0.07	0.09	0.05	0.05	0.07	0.07	0.09
F6	0.05	0.05	0.06	0.06	0.07	0.05	0.05	0.06	0.06	0.07
F7	0.08	0.08	0.10	0.12	0.15	0.08	0.08	0.10	0.12	0.15
F8	0.08	0.08	0.11	0.12	0.15	0.08	0.08	0.11	0.12	0.15
<b>F9</b>	0.08	<b>0.08</b>	0.11	<b>0.12</b>	0.16	0.08	<b>0.09</b>	0.11	<b>0.13</b>	0.16
<b>F10</b>	<b>0.08</b>	0.09	0.11	0.13	0.17	<b>0.09</b>	0.09	0.11	0.13	0.17
F11	0.09	0.10	0.12	0.14	0.17	0.09	0.10	0.12	0.14	0.18
F12	0.07	0.08	0.10	0.10	0.13	0.07	0.08	0.10	0.10	0.13
F13	0.09	0.10	0.12	0.13	0.16	0.09	0.10	0.12	0.13	0.16
<b>F14</b>	0.07	<b>0.07</b>	0.09	0.10	<b>0.11</b>	0.07	<b>0.08</b>	0.09	0.10	<b>0.13</b>
F15	0.10	0.11	0.13	0.14	0.17	0.10	0.11	0.13	0.14	0.17
F16	0.07	0.07	0.09	0.10	0.11	0.07	0.07	0.09	0.10	0.11
F17	0.10	0.11	0.13	0.14	0.19	0.10	0.11	0.13	0.14	0.19
F18	0.07	0.08	0.09	0.11	0.12	0.07	0.08	0.09	0.11	0.12

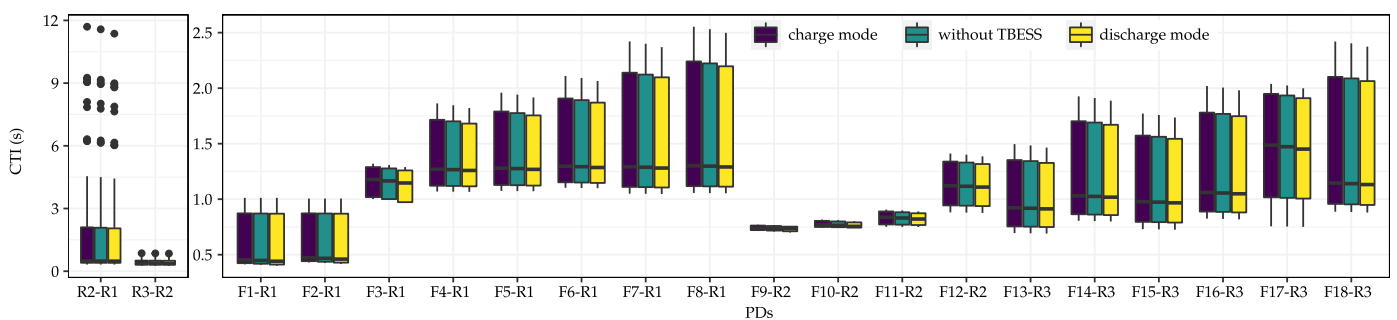


**Figure 6.** Boxplot of the CTIs obtained between the PDs with and without the TBESS (feeder #2).

### 3.3. Analysis of Feeder #3

Due to the large data volume, only the faults with the most significant impact are shown for this feeder. Tables 8 and 9 display the operating times of the PDs where there is a difference between the presence and absence of the TBESS. Table 8 shows that the differences are generally small, with significant changes only for faults involving fuse F18, which already has a long operating time as it is a 200K fuse. Similarly, Table 9 shows a shorter operating time with the battery system present. Notably, fuse F28 is not sensitized in any situation. Although it has the same capacity as fuse F18, the fault current of fuse F28 is lower than its triggering current due to its greater distance from the substation.

**Table 8.** Statistical evaluation of the operating times of PDs with and without the TBESS in charging mode (feeder #3).

PD	Operating Time (s)									
	With TBESS					Without TBESS				
	Min.	25th Perc.	50th Perc.	75th Perc.	Max.	Min.	25th Perc.	50th Perc.	75th Perc.	Max.
R1	<b>0.33</b>	<b>0.65</b>	1.07	<b>1.17</b>	<b>4.30</b>	<b>0.32</b>	<b>0.64</b>	1.07	<b>1.16</b>	<b>4.28</b>
R2	0.34	0.66	<b>0.84</b>	1.10	<b>4.29</b>	0.34	0.66	<b>0.83</b>	1.10	<b>4.25</b>
R3	0.29	0.49	0.79	0.87	<b>1.66</b>	0.29	0.49	0.79	0.87	<b>1.65</b>
R4	0.13	0.37	0.60	0.67	<b>1.36</b>	0.13	0.37	0.60	0.67	<b>1.35</b>
F18	<b>127.2</b>	<b>162.0</b>	<b>216.1</b>	<b>345.4</b>	<b>532.7</b>	<b>123.6</b>	<b>158.3</b>	<b>210.6</b>	<b>332.0</b>	<b>442.4</b>
F19	0.05	0.05	<b>0.07</b>	0.07	0.09	0.05	0.05	<b>0.06</b>	0.07	0.09
F79	0.06	<b>0.07</b>	0.08	0.09	0.13	0.06	<b>0.06</b>	0.08	0.09	0.13

**Table 9.** Statistical evaluation of the operating times of PDs with and without the TBESS in discharge mode (feeder #3).

PD	Operating Time (s)									
	With TBESS					Without TBESS				
	Min.	25th Perc.	50th Perc.	75th Perc.	Max.	Min.	25th Perc.	50th Perc.	75th Perc.	Max.
R1	<b>0.31</b>	<b>0.63</b>	1.07	1.16	<b>4.24</b>	<b>0.32</b>	<b>0.64</b>	1.07	1.16	<b>4.28</b>
R2	0.34	<b>0.64</b>	0.83	<b>1.09</b>	<b>4.20</b>	0.34	<b>0.66</b>	0.83	<b>1.10</b>	<b>4.25</b>
R3	<b>0.30</b>	<b>0.48</b>	<b>0.77</b>	<b>0.86</b>	<b>1.63</b>	<b>0.29</b>	<b>0.49</b>	<b>0.79</b>	<b>0.87</b>	<b>1.65</b>
R4	0.13	<b>0.36</b>	<b>0.59</b>	0.67	<b>1.33</b>	0.13	<b>0.37</b>	<b>0.60</b>	0.67	<b>1.35</b>
R5	<b>0.11</b>	<b>0.23</b>	<b>0.36</b>	0.42	<b>0.46</b>	<b>0.12</b>	<b>0.24</b>	<b>0.37</b>	0.42	<b>0.47</b>
F9	0.05	0.05	<b>0.05</b>	0.06	0.07	0.05	0.05	<b>0.06</b>	0.06	0.07
F18	<b>117.9</b>	<b>152.6</b>	<b>202.1</b>	<b>313.1</b>	<b>392.3</b>	<b>123.6</b>	<b>158.3</b>	<b>210.6</b>	<b>332.0</b>	<b>442.4</b>
F20	0.05	0.05	0.06	0.07	<b>0.09</b>	0.05	0.05	0.06	0.07	<b>0.10</b>
F21	0.05	0.05	0.06	0.07	<b>0.09</b>	0.05	0.05	0.06	0.07	<b>0.10</b>
F29	0.05	0.05	<b>0.05</b>	0.06	0.07	0.05	0.05	<b>0.06</b>	0.06	0.07
F33	0.06	0.06	<b>0.07</b>	0.08	0.10	0.06	0.06	<b>0.08</b>	0.08	0.10
F36	0.08	0.09	<b>0.10</b>	0.12	0.15	0.08	0.09	<b>0.11</b>	0.12	0.15
F49	0.05	0.06	0.07	0.11	<b>0.14</b>	0.05	0.06	0.07	0.11	<b>0.15</b>
F71	0.06	0.06	<b>0.06</b>	0.07	0.08	0.06	0.06	<b>0.07</b>	0.07	0.08
F72	0.06	0.07	<b>0.08</b>	0.11	0.15	0.06	0.07	<b>0.09</b>	0.11	0.15
F75	0.05	0.05	<b>0.05</b>	0.06	0.07	0.05	0.05	<b>0.06</b>	0.06	0.07

Figure 7 shows the CTIs between the PDs that exhibited the most significant variations. The largest intervals are observed between fuses F36 and F38 with recloser R2. Additionally, there is a lack of selectivity between certain fuses, such as F18, F19, F20, and F27 with F17; F21 with F20; F22 and F23 with F21; F25 and F26 with F24; F40 with F39; F46 with F45; F48 with F47; and F80 with F79. Some fault types also show selectivity loss between R2 and R1. However, the impact of the TBESS allocation in the substation is minimal, as the differences in CTIs with and without the system are small.

The analysis of feeder #3 PDs also showed a minor impact of the TBESS on operating times and selectivity. Based on the results from all the feeders simulated, it is possible to notice a small impact on the PDs overall. These results provide more confidence for future works proposing solutions for DS challenges, such as peak shaving, as the TBESS connection does minor harm to PDs operation. This technology can limit its current contribution during short-circuits, and the PDs operating time difference is negligible for the majority of short-circuit scenarios.

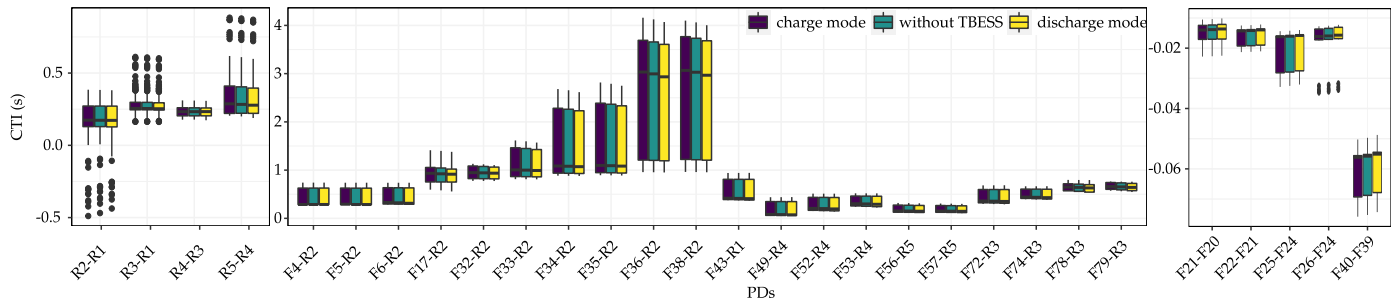


**Figure 7.** Boxplot of the CTIs obtained between the PDs with and without the TBESS (feeder #3).

#### 4. Conclusions

This study investigated the influence of a TBESS on the protection systems of a real-world distribution network. Specifically, the research explored how the connection and operation (charging or discharging) of a TBESS could affect the coordination and functionality of the existing PDs such as reclosers and fuses. This comprehensive analysis aimed to determine whether TBESS integration would necessitate adjustments to the protection schemes in place. The key findings of the study are as follows:

- *Minimal Impact on Operating Times:* The integration of a TBESS resulted in only minor variations in the operating times of PDs across different feeders. These variations were generally within hundredths of a second, indicating a negligible impact on the overall performance and coordination of the protection system. This suggests that the existing protection settings are sufficiently robust to handle the inclusion of a TBESS without significant disruption.
- *No Need for Modifications:* Based on the results, no modifications are required for the protection system to accommodate a TBESS in the analyzed substation. This implies that the current protection infrastructure can seamlessly integrate a TBESS, maintaining system reliability and operational integrity.
- *Consideration for Mobility:* Due to the mobility feature of TBESSs, it is recommended to examine protection issues during the planning stages of TBESS connections at other substations and feeders. Each new location may present unique challenges that need to be addressed to ensure seamless integration and optimal performance.
- *Utility Perspective:* From the utilities' perspective, the findings are significant because they suggest that no alterations in the protection system are necessary for connecting a TBESS at the investigated feeders. This can facilitate quicker deployment and operationalization of TBESSs in the grid, reducing the time and cost associated with system modifications.
- *Future Analyses and Contributions:* The outcomes and methodologies presented in this paper are valuable for future analyses concerning the allocation of TBESSs in DSs. They provide a robust foundation for further research and practical applications, ensuring that the integration of TBESSs contributes to more resilient and adaptable power networks with minor adaptations. This study's findings can guide utilities and researchers in assessing the potential impacts of TBESSs on different systems, fostering a smoother transition to advanced energy storage solutions.
- *Scalability:* Although the study was limited to three real feeders, the results indicate a trend that TBESS integration presents minimal impacts on protection systems. It is recommended that each system be analyzed individually to account for specific characteristics and potential variations. However, the indicative trend of minimal impact is promising and suggests that widespread TBESS deployment could be feasible with similar results.

In conclusion, the study demonstrates that TBESSs can be integrated into existing distribution networks with minimal impact on protection systems, thereby supporting the transition to more flexible and reliable power grids. The research underscores the importance of evaluating each system individually, particularly given the mobility of TBESSs, but

the overall trend is encouraging for broader deployment. This study lays a foundation for future research and practical applications, supporting the strategic integration of TBESSs into modern power networks.

**Author Contributions:** Conceptualization, A.E.C.M., P.H.A.B. and P.I.N.B.; methodology, A.E.C.M., P.H.A.B. and P.I.N.B.; software, A.E.C.M., P.H.A.B. and P.I.N.B.; validation, A.E.C.M., P.H.A.B. and P.I.N.B.; formal analysis, A.E.C.M., P.H.A.B. and P.I.N.B.; investigation, A.E.C.M., P.H.A.B. and P.I.N.B.; writing—original draft preparation, A.E.C.M., P.H.A.B. and P.I.N.B.; writing—review and editing, A.E.C.M., P.H.A.B., P.I.N.B., E.N.A., J.C.M.V. and D.V.C.; supervision, E.N.A., J.C.M.V. and D.V.C. All authors have read and agreed to the published version of the manuscript.

**Funding:** This work was supported in part by the Coordenação de Aperfeiçoamento de Pessoal de Nível Superior-Brasil (CAPES)–Finance Code 001, and by the Conselho Nacional de Desenvolvimento Científico e Tecnológico (CNPq) through Project 402334/2023-0. Additionally, doctoral research funding was provided by Processes 140235/2021-3 and 445374/2020-9. This work also received support from the Chamada Interna de Apoio à Pesquisa N° 02/PROPEQ/2024 -Apoio à Publicação em Periódicos Qualificados (UFMT) and the Program for Research and Technological Development of the Electric Energy Sector regulated by ANEEL, Brazil: R&D Number 2866–0454/2016–Transportable Storage System to Support Scheduled Contingencies at Substations—a partnership among EESC-USP, CPqD and COPEL S.A.

**Data Availability Statement:** Data are contained within the article.

**Conflicts of Interest:** The authors declare no conflicts of interest.

## Abbreviations

The following abbreviations are used in this manuscript:

BESS	Battery energy storage system
CTI	Coordination time interval
DS	Distribution system
ESS	Energy storage system
PD	Protection device
TBESS	Transportable battery energy storage system
VSC	Voltage-sourced converter

## References

- Mao, J.; Jafari, M.; Botterud, A. Planning low-carbon distributed power systems: Evaluating the role of energy storage. *Energy* **2022**, *238*, 121668. [CrossRef]
- Jafari, M.; Korpås, M.; Botterud, A. Power system decarbonization: Impacts of energy storage duration and interannual renewables variability. *Renew. Energy* **2020**, *156*, 1171–1185. [CrossRef]
- Hannan, M.; Wali, S.; Ker, P.; Rahman, M.A.; Mansor, M.; Ramchandaramurthy, V.; Muttaqi, K.; Mahlia, T.; Dong, Z. Battery energy-storage system: A review of technologies, optimization objectives, constraints, approaches, and outstanding issues. *J. Energy Storage* **2021**, *42*, 103023. [CrossRef]
- Yang, Y.; Bremner, S.; Menictas, C.; Kay, M. Battery energy storage system size determination in renewable energy systems: A review. *Renew. Sustain. Energy Rev.* **2018**, *91*, 109–125. [CrossRef]
- J. Eyer and G. Corey. Energy Storage for the Electricity Grid: Benefits and Market Potential Assessment Guide. Technical Report, 2010. Available online: <https://www.sandia.gov/ess-ssl/publications/SAND2010-0815.pdf> (accessed on 22 July 2024).
- Zuo, W.; Zhang, Y.; E, J.; Li, J.; Li, Q.; Zhang, G. Performance comparison between single S-channel and double S-channel cold plate for thermal management of a prismatic LiFePO<sub>4</sub> battery. *Renew. Energy* **2022**, *192*, 46–57. [CrossRef]
- Abdeltawab, H.H.; Mohamed, Y.A.I. Mobile Energy Storage Scheduling and Operation in Active Distribution Systems. *IEEE Trans. Ind. Electron.* **2017**, *64*, 6828–6840. [CrossRef]
- Lei, S.; Chen, C.; Zhou, H.; Hou, Y. Routing and Scheduling of Mobile Power Sources for Distribution System Resilience Enhancement. *IEEE Trans. Smart Grid* **2019**, *10*, 5650–5662. [CrossRef]
- Kim, J.; Dvorkin, Y. Enhancing Distribution System Resilience With Mobile Energy Storage and Microgrids. *IEEE Trans. Smart Grid* **2019**, *10*, 4996–5006. [CrossRef]
- Mirzaei, M.A.; Hemmati, M.; Zare, K.; Mohammadi-Ivatloo, B.; Abapour, M.; Marzband, M.; Razzaghi, R.; Anvari-Moghaddam, A. Network-constrained rail transportation and power system scheduling with mobile battery energy storage under a multi-objective two-stage stochastic programming. *Int. J. Energy Res.* **2021**, *45*, 18827–18845. [CrossRef]

11. Ebadi, R.; Sadeghi Yazdankhah, A.; Mohammadi-Ivatloo, B.; Kazemzadeh, R. Coordinated power and train transportation system with transportable battery-based energy storage and demand response: A multi-objective stochastic approach. *J. Clean. Prod.* **2020**, *275*, 123923. [CrossRef]
12. Ebadi, R.; Sadeghi Yazdankhah, A.; Kazemzadeh, R.; Mohammadi-Ivatloo, B. Techno-economic evaluation of transportable battery energy storage in robust day-ahead scheduling of integrated power and railway transportation networks. *Int. J. Electr. Power Energy Syst.* **2021**, *126*, 106606. [CrossRef]
13. Hayajneh, H.S.; Zhang, X. Logistics Design for Mobile Battery Energy Storage Systems. *Energies* **2020**, *13*, 1157. [CrossRef]
14. Saboori, H.; Jadid, S.; Savaghebi, M. Optimal Management of Mobile Battery Energy Storage as a Self-Driving, Self-Powered and Movable Charging Station to Promote Electric Vehicle Adoption. *Energies* **2021**, *14*, 736. [CrossRef]
15. Wang, Y.; Rousis, A.O.; Strbac, G. Resilience-driven optimal sizing and pre-positioning of mobile energy storage systems in decentralized networked microgrids. *Appl. Energy* **2022**, *305*, 117921. [CrossRef]
16. Wang, Y.; Qiu, D.; Strbac, G. Multi-agent deep reinforcement learning for resilience-driven routing and scheduling of mobile energy storage systems. *Appl. Energy* **2022**, *310*, 118575. [CrossRef]
17. Mishra, D.K.; Ghadi, M.J.; Li, L.; Zhang, J.; Hossain, M. Active distribution system resilience quantification and enhancement through multi-microgrid and mobile energy storage. *Appl. Energy* **2022**, *311*, 118665. [CrossRef]
18. Saboori, H.; Jadid, S. Capturing curtailed renewable energy in electric power distribution networks via mobile battery storage fleet. *J. Energy Storage* **2022**, *46*, 103883. [CrossRef]
19. Dantas, N.K.L.; Souza, A.C.M.; Vasconcelos, A.S.M.; Junior, W.d.A.S.; Rissi, G.; Dall’Orto, C.; Maciel, A.M.A.; Castro, J.F.C.; Liu, Y.; Rosas, P. Impact Analysis of a Battery Energy Storage System Connected in Parallel to a Wind Farm. *Energies* **2022**, *15*, 4586. [CrossRef]
20. Caldeira, C.A.; de Almeida, A.D.D.; Schlickmann, H.R.; Gehrke, C.S.; Salvadori, F. Impact analysis of the BESS insertion in electric grid using real-time simulation. In Proceedings of the 2019 IEEE PES Innovative Smart Grid Technologies Conference—Latin America (ISGT Latin America), Gramado, Brazil, 15–18 September 2019; pp. 1–6. [CrossRef]
21. Boloorch, M.; Rostami, M.; Green, V. BESS connection impact assessment. In Proceedings of the 2017 IEEE 30th Canadian Conference on Electrical and Computer Engineering (CCECE), Windsor, ON, Canada, 30 April–3 May 2017; pp. 1–4. [CrossRef]
22. Feng, Y.; Zhang, Z.; Lai, Q.; Yin, X.; Liu, H. Impact of Inverter Interfaced Generators on Distance Protection. In Proceedings of the 2019 4th International Conference on Intelligent Green Building and Smart Grid (IGBSG), Yichang, China, 6–9 September 2019; pp. 512–515. [CrossRef]
23. Haddadi, A.; Farantatos, E.; Kocar, I.; Karaagac, U. Impact of Inverter Based Resources on System Protection. *Energies* **2021**, *14*. [CrossRef]
24. Momesso, A.E.C.; Barra, P.H.A.; Barbalho, P.I.N.; Asada, E.N.; Coury, D.V.; Vieira, J.C.M.; Oleskovicz, M.; Biczkowski, M. Impact Analysis of a Transportable BESS on the Short-Circuit Behavior in a Distribution System. In Proceedings of the 2020 IEEE Power Energy Society General Meeting (PESGM), Montreal, QC, Canada, 2–6 August 2020; pp. 1–5. [CrossRef]
25. *IEEE Std 1547-2018*; IEEE Standard for Interconnection and Interoperability of Distributed Energy Resources with Associated Electric Power Systems Interfaces. Revision of IEEE Std 1547-2003. IEEE: Piscataway, NJ, USA, 2018; pp. 1–138. [CrossRef]
26. S&C Electric Company. IntelliRupter PulseCloser Fault Interrupter: Outdoor Distribution (15 kV, 27 kV, and 38 kV): Time-Current Characteristic Curves. Information Bulletin. 2020. Available online: <https://www.sandc.com/globalassets/sac-electric/documents/public---documents/sales-manual-library---external-view/information-bulletin-766-211.pdf?dt=638168970269398694> (accessed on 22 July 2024).
27. S&C Electric Company. Type XS Fuse Cutout—For outdoor distribution, 4.16 kV through 25 kV. Information Bulletin. 2020. Available online: <https://www.sandc.com/en/products--services/products/type-xs-fuse-cutout/> (accessed on 22 July 2024).
28. Das, J.C. *Power System Protective Relaying*; CRC Press: Boca Raton, FL, USA, 2018.

**Disclaimer/Publisher’s Note:** The statements, opinions and data contained in all publications are solely those of the individual author(s) and contributor(s) and not of MDPI and/or the editor(s). MDPI and/or the editor(s) disclaim responsibility for any injury to people or property resulting from any ideas, methods, instructions or products referred to in the content.